small NANO MICRO

Nanoassemblies

DOI: 10.1002/smll.200700731

Discovery of New Hexagonal Supramolecular Nanostructures Formed by Squalenoylation of an Anticancer Nucleoside Analogue

Patrick Couvreur, L. Harivardhan Reddy, Stéphanie Mangenot, Jacques H. Poupaert, Didier Desmaële, Sinda Lepêtre-Mouelhi, Barbara Pili, Claudie Bourgaux, H. Amenitsch, and Michel Ollivon*

We dedicate this manuscript to the memory of our beloved colleague and scientist Dr. Michel Ollivon, recently deceased.

In this study, the dynamically folded conformation of squalene (SQ) is taken advantage of to link this natural compound to the anticancer nucleoside analogue gemcitabine (gem) in order to achieve the spontaneous formation of nanoassemblies (SQgem) in water. Cryogenic transmission electron microscopy examination reveals particles (104 nm) with a hexagonal or multifaceted shape that display an internal structure made of reticular planes, each particle being surrounded by an external shell. X-ray diffraction evidences the hexagonal molecular packing of SQgem, resulting from the stacking of direct or inverse cylinders. The respective volumes of the gem and SQ molecules as well as molecular modeling of SQgem suggest the stacking of inverse hexagonal phases, in which the central aqueous core, consisting of water and gem molecules, is surrounded by SQ moieties. These SQgem nanoassemblies also exhibit impressively greater anticancer activity than gem against a solid subcutaneously grafted tumor, following intravenous administration. To our knowledge, this is the first demonstration of hexagonal phase organization with a SQ derivative.

Keywords:
- antitumor agents
- gemcitabine
- squalene
- structure elucidation
- supramolecular assembly

[*] Prof. P. Couvreur, L. H. Reddy, B. Pili, C. Bourgaux, Dr. M. Ollivon†
Université Paris-Sud XI, Faculté de Pharmacie
UMR CNRS 8612, IFR 141
92296 Châtenay-Malabry Cedex (France)
Fax: (+33) 146-619-334
E-mail: patrick.couvreur@cep.u-psud.fr

S. Mangenot
Université Paris-Sud, Laboratoire de Physique des Solides
91405 Orsay (France)

J. H. Poupaert
Unité de Chimie Pharmaceutique et Radiopharmacie
Université Catholique de Louvain
1200 Bruxelles (Belgium)

D. Desmaële, S. Lepêtre-Mouelhi
Université Paris-Sud XI, Faculté de Pharmacie
UMR CNRS 8076 Biocis
92296 Châtenay-Malabry Cedex (France)

H. Amenitsch
Elettra sincrotrone
34012 Basovizza, Trieste (Italy)

1. Introduction

Squalene (SQ) is a natural acyclic molecule that has the unique property of being transformed into the cyclic derivative lanosterol (a precursor of cholesterol) by spontaneously passing through a highly coiled, compact conformation, without the aid of either coenzymes or biochemical energy (ATP).[1,2] The flexibility of SQ and SQ derivatives and the possibility of assuming many different conformations with similar stability certainly help these molecules in reaching the hydrophobic pocket of the enzyme (i.e., oxidosqualene cyclase) in which the cyclization occurs.[3] SQ is abundant in shark liver oil; this lipid is also distributed ubiquitously in human tissues, and at greater concentrations in the skin.[4] Because of the nontoxic and biocompatible characteristics of squalene, we have used this natural lipid as a carrier for the delivery of nucleoside analogues (NAs).[5] Of the various nucleoside analogues available, the pyrimidine NAs (gemci-

tabine and cytarabine) represent a group of cytotoxic agents with high activity in lymphoid and myeloid malignancies, as well as in solid tumours, including colon, lung, pancreatic, breast, bladder, and ovarian cancers.[6,7] However, gemcitabine (gem), like cytarabine, exhibits certain drawbacks like rapid metabolization, intracellularly and extracellularly by deoxycytidine deaminase (deamination), into the chemotherapeutically inactive uracil derivative, leading to a short plasma half-life (1.5 h) and drug resistance.[8] In this context, we developed a new medicine based on the nanoscale, namely, 4-(*N*)-trisnorsqualenoylgemcitabine (SQgem), by covalent coupling of gemcitabine to squalene.

2. Results and Discussion

The synthesis of SQgem began with the oxidation of the C27 squalene aldehyde into 1,1',2-trisnorsqualenic acid, which was then activated with ethyl chloroformate before coupling to gemcitabine. The obtained 4-(*N*)-trisnorsqualenoylgemcitabine was characterized by ^{1}H and ^{13}C NMR, IR, elemental analysis, and mass spectroscopy (electrospray ionization: MS-ESI), confirming the structure of the expected molecule. Thus, following this procedure, a selective 4-acylation of gemcitabine was obtained.

The SQgem nanoassemblies were obtained in a single step by straightforward precipitation from an ethanolic solution of SQgem in water or 5% aqueous dextrose solution. The mean diameter of the obtained nanoassemblies was found to be 125 ± 8 nm with a unimodal size distribution (0.1) as measured by quasi-elastic light scattering.

2.1. Cryogenic Transmission Electron Microscopy

SQgem nanoassemblies were then vitrified and imaged by cryogenic transmission electron microscopy (cryoTEM, Figure 1). Depending on the nanoassembly and its orientation, they presented a hexagonal or multifaceted shape with size ranging from 27 to 125 nm and an average value (in weight) of approximately 104 nm (Figure 1A and B). Of note is that the cryoTEM does not take into account the particles with a diameter larger than 300 nm. Each nanoassembly was surrounded by an external shell (approximately 3.27 nm thick) and displayed an internal structure made of reticular planes. When the nanoassemblies were oriented in the appropriate direction (Figure 1B), they clearly exhibited a sixfold symmetry, as displayed by the Fourier transform, with a distance of approximately 5.2 nm between the different planes (Figure 1D). In some cases, reticular planes were visible with a repeat distance of 4.67 ± 0.02 nm as displayed on Figure 1A and the corresponding Fourier transform of the assemblies (Figure 1C).

2.2. X-ray Diffraction Studies

Nanoassemblies were concentrated by ultracentrifugation and examined by X-ray diffraction at both small and wide angles. At room temperature, this obtained phase exhibited hexagonal packing as shown by Bragg reflections observed at small angles, whose positions are in characteristic ratios ($1:\sqrt{3}:\sqrt{4}:\sqrt{7}:\sqrt{9}:\sqrt{12}:\sqrt{13}$) (Figure 2A). This phase displayed the lattice parameter $a = 8.77 \pm 0.02$ nm at room temperature (RT). Two very weak and broad lines were observed at wide angles ($q = 1.33$ Å^{-1} and $q = 1.53$ Å^{-1}). SQgem is a long chain (C27) amphiphilic molecule, which is expected to form mesophases upon hydration. The hexagonal phase evidenced above resulted from the stacking of direct or inverse cylinders. The respective volumes occupied by the chain (about 720 Å^3) and the hydrated polar group (350 Å^3) suggest the packing of SQgem in an inverted hexagonal phase (Figure 2B). Moreover, the stability of the nanoassemblies in excess aqueous phase is in favor of an inverted structure. Water plus gem columns were surrounded by SQ moieties, as shown schematically in Figure 2C. The observed difference in the distance between the centers of columns measured by cryoTEM (5.2 nm) and by X-ray diffraction (8.77 nm) might have resulted from the sample preparation procedure for cryoTEM observation (i.e., dehydration as a consequence of sample preparation and/or slight structural change upon cooling). The presence of the six additional spots as seen in the Fourier transform of Figure 1D could be due to a defect in the hexagonal bundle of lipid rods, such as a screw dislocation. On heating, an endothermic peak was recorded at about 40°C, weak wide-angle lines disappeared, and the hexagonal phase transformed into a cubic-like phase (data not shown). The transition was not reversible and cooling to 0°C did not re-

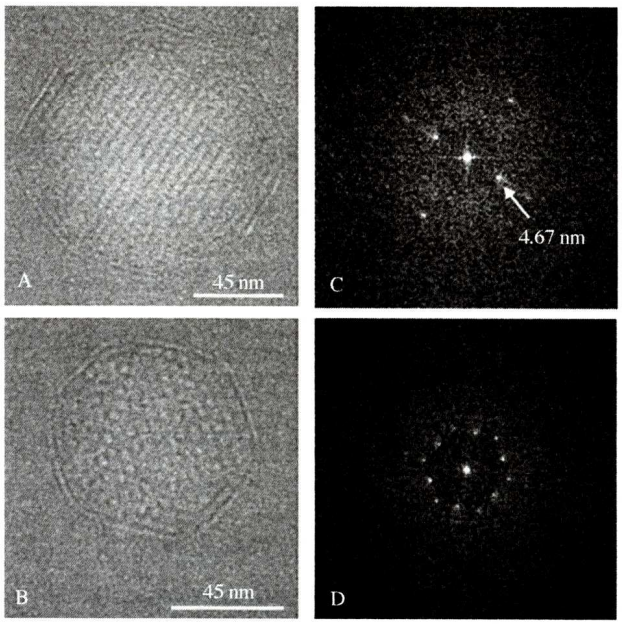

Figure 1. CryoTEM images of nanoassemblies of 4-(*N*)-trisnorsqualenoylgemcitabine. The supramolecular organization is clearly visible. Nanoassemblies of hexagonal shape (A and B) are surrounded by an external shell and display an internal structure. The Fourier transforms of (A) and (B) assessed by ImageJ software reveal a hexagonal symmetry (D) between columns with a 4.67-nm periodicity (C).

NANO MICRO small

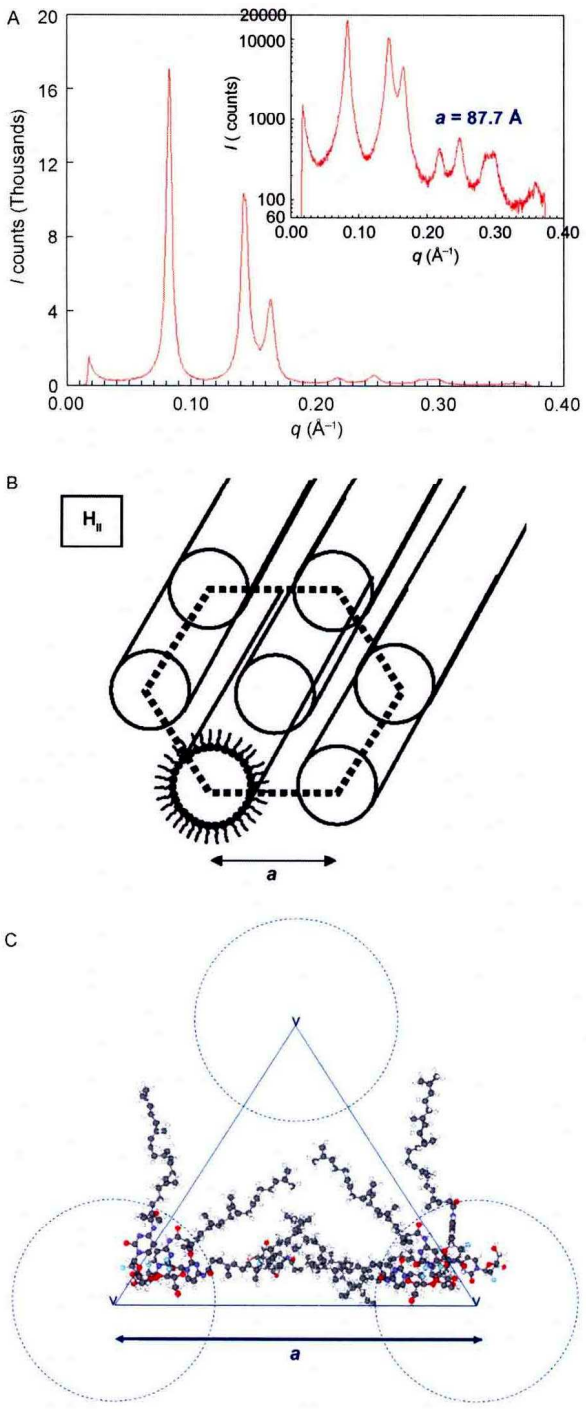

Figure 2. A) Small-angle X-ray scattering patterns of the hexagonal phase shown on both linear and log (inset) scales, with Bragg lines at $1:\sqrt{3}:\sqrt{4}:\sqrt{7}:\sqrt{9}:\sqrt{12}:\sqrt{13}$. B) Schematic drawing of the hexagonal (H_{II}) packing of amphiphilic molecules. C) Molecules are arranged along water channels containing hydrophilic moieties. The respective volumes of lipophilic and hydrophilic moieties of SQgem favor the reverse packing drawn with about 12–14 molecules per equilateral triangular unit.

store the high-temperature phase to the initial hexagonal phase. The complex thermal and structural behavior of SQgem will be analysed in a forthcoming paper.

2.3. Molecular Modeling

Molecular modeling studies of the SQgem were therefore undertaken to understand its mode of association and supramolecular organization. A conformation search on SQgem was performed by a combined approach of molecular dynamics and energy minimization using AM1, and further refined using a hypergeometric-type function (HTF) quantum-mechanics method with a 6-31G** basis set as implemented in Gaussian03.[9] Two families of conformers were evidenced: the first one with an extended conformation and the second one with a bent U-shape conformation, both with relatively similar free enthalpy (ΔHf). The energy minima of each family were then found using a HTF quantum-mechanics method and a 6-31G** basis set. In these conditions, the linear conformer was found to have a slightly energy-favored (binding energy difference: 1.2 kcal mol^{-1}) conformation. This conformation is very similar to that observed in the squalene crystal by Ernst et al.[10] Using the low-energy extended conformer structure and the information obtained by X-ray diffraction, a disk-like assembly composed of 20 conjugates was initially created with the heterocyclic polar tetrahydrofuran moiety facing inwards and the squalene lipophilic side chain facing outwards. As this system was too big to be calculated by AM1 in its totality, it was energy-minimized sequentially by pairs of conju-

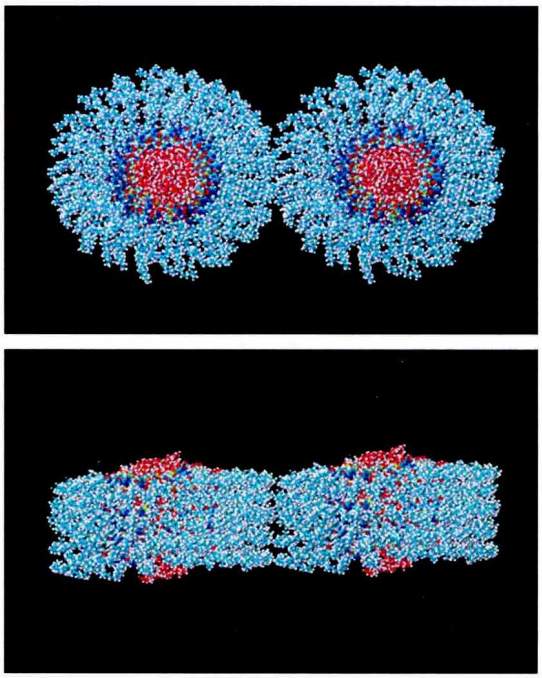

Figure 3. Face (upper part) and top (lower part) views of a construction of two sections of column, each made of six layers of a disk-like assembly composed of 20 conjugates. The whole system encompasses 31 178 atoms with 240 conjugates and 2556 water molecules. On the face view, the aqueous core is clearly visible in the center (oxygen/red), and the extent of the polar heterocyclic part can be appreciated by the presence of a circle of pyrimidinone nitrogen atoms (blue) and fluorine atoms (yellow). The top view shows the central inclusion of the water spindle surrounded by lipophilic squalene side chains.

gates (see Experimental Section). Subsequently, a column system consisting of six superposed disks was constructed (i.e., 120 conjugates) and rapidly energy-minimized using the optimized potentials for liquid simulations (OPLS) force field. A water spindle was then inserted in the polar core of the system. Two such columns were then positioned with a distance of 87.7 Å between the centers of the aqueous core. The whole system shown in Figure 3 encompasses 31 178 atoms with 240 conjugates and 2556 water molecules. Essentially, the interstitial region between columns must be filled with the hydrocarbon chains,[11] implying that some chains have either to stretch from their preferred conformation or be compressed (see representation in Figure 2C). It is also interesting that the water molecules were strongly hydrogen-bonded to each other but made few interactions with the central polar heterocyclic surround. Moreover, no diffusion of water molecules was observed within the heterocyclic surrounds.

Overall, these data show that the 4-(*N*)-trisnorsqualenoylgemcitabine molecules self-assemble as nanoassemblies made of inverse hexagonal phases; the cohesion of the nanoassemblies resulting mainly from hydrophobic forces and hydrogen bonds at the level of amide of the pyrimidinone moiety or between fluorine atoms and the exocyclic $-CH_2-OH$ moieties, the central aqueous core assuring further cohesion of the whole system. When Langevin dynamics was performed on this system (320 K, OPLS), the system slowly evolved to a globular structure. This behavior occurred in parallel with the phase transition observed upon heating.

2.4. In vivo Anticancer Activity Studies

Following the structural elucidation, the SQgem nanoassemblies were tested for their anticancer activity and compared with gem after intravenous administration to P388 subcutaneous-tumour-bearing mice. Compared with all the other treatments, such as those with saline and gem, the SQgem nanoassembly treatment caused significant control over the tumour growth in mice ($P<0.05$) (Figure 4A and C). The same results were reflected from the survival curves constructed for untreated and treated groups. The survival curve of the gemcitabine-treated group was similar to that of the untreated and saline-treated groups, whereas the SQgem nanoassembly-treated group exhibited significantly longer survival of the tumour-bearing mice (Figure 4B). These data clearly indicate the greater anticancer efficiency of SQgem nanoassemblies compared with gem. To further investigate the mechanism behind the superiority of the anticancer activity of SQgem nanoassemblies comparative to gemcitabine, a P388 ascitis mice model was developed by growing the P388 leukemia cells in the peritoneal cavity. Three days after intravenous injection of either gem (10 mg kg^{-1}) or SQgem (10 mg kg^{-1} equivalent of gem), the ascitic cells were collected and studied for cell-cycle events, especially the percentage of cells in S-phase and apoptosis by measuring the sub-G0/G1 population. The SQgem treatment exhibited greater specificity than the gem treatment to

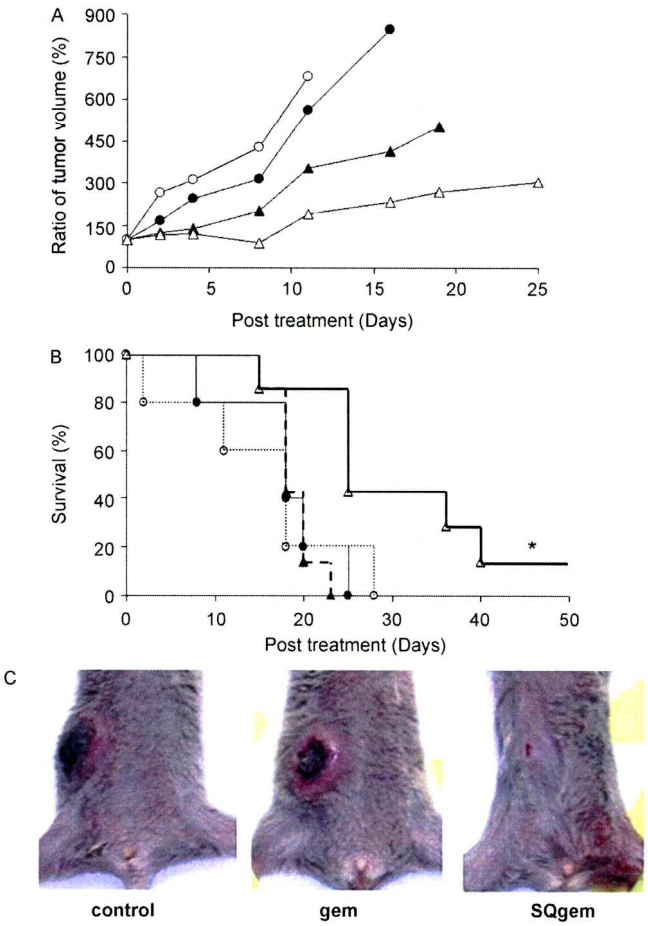

Figure 4. Anticancer activity of SQgem in nanoassembly form and gem (5 mg kg^{-1} equivalent doses) following intravenous treatment (on days 0, 4, 8, and 13) of mice bearing P388 subcutaneous tumours. A) Tumour progression: Control (black spheres), saline (white spheres), gem (black diamonds), SQgem nanoassemblies (white diamonds). B) Survival curve of mice: Control (solid line), saline (dotted line), gem (dashed line), SQgem nanoassemblies (heavy solid line). * indicates $P<0.05$, as assessed by Kaplan–Meier test. C) Photograph showing the difference in tumour growth in mice following the completion of indicated treatment.

the S-phase cells, causing greater S-phase arrest and higher apoptosis (Figure 5). These results clearly show that the SQgem is more active against cancer following intravenous treatment and is also more effective at the cellular level, causing greater cell kill than free gem, and, hence, it could be advantageous in the treatment of cancer.

3. Conclusions

In conclusion, this study clearly demonstrates that the internal organization at the supramolecular scale of nanoassemblies of SQgem at room temperature is hexagonal with a parameter $a = 8.8$ nm between hydrophilic columns. To our knowledge this is the first demonstration of hexagonal phase organization with a squalene derivative. While squalenoylation is an original technology platform for generating more potent anticancer nanometer-scale medicines, the rela-

NANO MICRO small

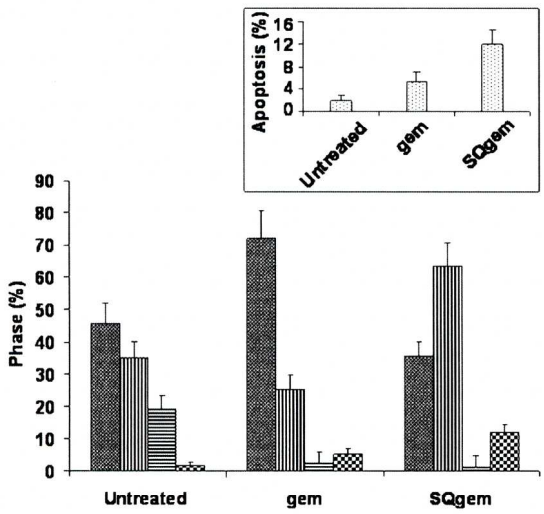

Figure 5. Effect of gem and of SQgem nanoassemblies on the P388 leukemia cells collected from ascitis-bearing mice following three days post intravenous injection (10 mg kg^{-1} gem or 10 mg kg^{-1} SQgem equivalent of gem) ($n = 3$). G0/G1 phase (small hatching), S-phase (vertical stripes), G2/M phase (horizontal stripes), apoptotic phase (large hatching). The top-right corner box depicts an enlarged view of the apoptotic phase.

tionship between the drug efficiency and the internal structure of the nanoassemblies warrants further investigation.

4. Experimental Section

Gemcitabine hydrochloride was purchased from Sequoia Research Products (UK). Squalene, dextrose, and dimethylsulfoxide were purchased from Sigma–Aldrich (France).

Synthesis of 4-(N)-Trisnorsqualenoylgemcitabine (SQgem): Triethylamine (0.15 g, 1.4 mmol) was added, under nitrogen, to a stirred solution of trisnorsqualenoic acid (0.50 g, 1.2 mmol) in anhydrous tetrahydrofuran (THF) (4 mL). The mixture was cooled to 0°C, and ethyl chloroformate (0.135 g, 1.2 mmol) in anhydrous THF (3 mL) was added dropwise. The mixture was stirred at 0°C for 15 min, and a solution of gemcitabine hydrochloride (0.37 g, 1.2 mmol) and triethylamine (0.15 g, 1.4 mmol) in anhydrous dimethylformamide (DMF) (5 mL) was added dropwise to the reaction at the same temperature. The reaction was stirred for 72 h at room temperature, and the reaction mixture was concentrated in vacuo. The crude product was purified by chromatography on silica gel (CH_2Cl_2/MeOH/Et_3N, 95:5:0.5). The collected fractions were concentrated in vacuo. The residue was taken into ethyl acetate, washed with water, dried, and concentrated to give eluting with 1 to 5% methanol in dichloromethane to give pure 4-(*N*)-trisnorsqualenoylgemcitabine as an amorphous white solid (0.46 g, 57%). $[\alpha]_D = 3.1^\circ\ cm^3\ g^{-1}$ ($c = 0.95\ g\ cm^{-3}$, CH_2Cl_2); ^1H NMR (300 MHz, $CDCl_3$, δ): 9.15 (broad s, 1H, NHCO), 8.16 (d, 1H, $J = 7.5$ Hz, H6), 7.47 (d, 1H, $J = 7.5$ Hz, H5), 6.18 (t, 1H, $J = 7.0$ Hz, H1′), 5.22–5.15 (m, 5H, *H*C=C-(CH_3)), 4.49 (m, 1H, H3′), 4.86–4.09 (m, 3H, H4′ and H5′), 2.55 (m, 2H), 2.38–2.28 (m, 2H), 2.13–1.91 (m, 16H, CH_2), 1.69–1.55 ppm (m, 18H, C=C(CH_3)); ^{13}C NMR (75 MHz, $CDCl_3$, δ): 173.7 (*C*ONH), 163.0 (HN*C*=N), 155.8 (N*C*ON), 145.4 (CH, C6), 135.1 (C), 134.9 (2 C), 132.7 (C), 131.2 (C), 125.7 (CH), 124.4 (2 CH), 124.2 (2 CH), 122.4 (CF_2), 97.7 (CH, C5), 81.7 (2 CH), 69.2 (CH), 59.9 (CH_2), 39.7 (2 CH_2), 39.5 (CH_2), 36.5 (CH_2), 34.3 (CH_2), 28.3 (2 CH_2), 26.8 (CH_2), 26.7 (CH_2), 26.6 (CH_2), 25.6 (CH_3), 17.6 (CH_3), 16.0 (3 CH_3), 15.8 ppm (CH_3); IR (neat, ν): 3500–3150, 2950, 2921, 2856, 1709, 1656, 1635, 1557, 1490, 1435, 1384, 1319, 1275, 1197, 1130, 1071 cm^{-1}; MS-ESI: $m/z = 644$ ($[M-H]^-$, 100%); Anal. Calcd for $C_{36}H_{53}N_3O_5$: C, 66.95, H, 8.27, N, 6.51. Found: C, 66.76, H, 8.40, N, 6.39.

Characterization: IR spectra were obtained from solids or neat liquid on a Fourier transform Bruker Vector 22 spectrometer. Only significant absorptions are listed. Optical rotations were measured on a Perkin–Elmer 241 polarimeter at 589 nm. The ^1H and ^{13}C NMR spectra were recorded on Bruker AC 200 P (200 MHz and 50 MHz, for ^1H and ^{13}C, respectively) or Bruker Avance-300 (300 MHz and 75 MHz, for ^1H and ^{13}C, respectively) spectrometers. Identification of methyl, methylene, methine, and quaternary carbon nuclei in ^{13}C NMR spectra was based on the *J*-modulated spin-echo sequence. Mass spectra were recorded on a Bruker Esquire-LC. Analytical thin-layer chromatography was performed on Merck silica gel $60F_{254}$ precoated glass plates (0.25 mm layer). Column chromatography was performed on Merck silica gel 60 (230–400 mesh ASTM). THF was distilled from sodium/benzophenone ketyl. Methanol was dried over magnesium and distilled. DMF, CH_2Cl_2, and triethylamine were distilled from calcium hydride under a nitrogen atmosphere. All reactions involving air- or water-sensitive compounds were routinely conducted in glassware, which was flame-dried under positive pressure of nitrogen. Elemental analyses were performed by the Service de Microanalyse, Centre d'Études Pharmaceutiques, Châtenay-Malabry, France, with a Perkin–Elmer 2400 analyzer. Chemicals obtained from commercial suppliers were used without further purification. Trisnorsqualenoic acid was prepared from squalene as per the method of Ceruti et al.[2]

Preparation and characterization of the squalenoyl nanoassemblies: SQgem nanoassemblies were prepared by precipitation. Briefly, 4-(*N*)-trisnorsqualenoylgemcitabine was dissolved in acetone (10 mg mL^{-1}). This solution was added dropwise under stirring (500 rpm) into a 5% aqueous dextrose solution. Precipitation of the nanoassemblies occurred spontaneously. Acetone was completely evaporated using a Rotavapor instrument to obtain an aqueous suspension of pure nanoassemblies (5 mg mL^{-1}).

The mean diameters of the nanoassemblies were determined at 20°C by quasi-elastic light scattering (QELS) using a nanosizer (Coulter N4MD, Coulter Electronics, Inc., Hialeah, FL). The selected angle was 90° and the measurement was made after dilution of the suspension of nanoassemblies in 5% aqueous dextrose solution.

Cryogenic transmission electron microscopy: SQgem nanoassemblies were vitrified using a chamber designed and set up in the laboratory where both humidity and tempera-

ture can be controlled. A 4 μL drop of the suspension of SQgem nanoassemblies (2 mg mL^{-1}) was deposited onto a perforated carbon film mounted on a 200 mesh electron microscopy grid. The home-made carbon film holes dimensions were about 2 μm in diameter. Most of the drop was removed with a blotting filter paper and the residual thin films remaining within the holes were vitrified after immersion in liquid ethane using a guillotine-like frame. The specimen was then transferred, using liquid nitrogen, to a cryo-specimen holder and observed using a JEOL FEG-2010 electron microscope. Micrographs were recorded at 200 kV under low-dose conditions at a magnification of 40 000 on SO-163 Kodak films. Micrographs were digitized using a film scanner (Super coolscan 8000 ED, Nikon), and analysis was made using the ImageJ software.

X-ray diffraction studies: SQgem nanoassemblies were ultracentrifuged (40 000 rpm, 4°C) and the sediment was obtained. This sediment phase was selectively sampled using a long-needle syringe specially developed for X-ray capillary preparation and about 25 mg of this phase was introduced into quartz capillaries. Briefly, the capillaries were first examined at room temperature using Microcalix as the sample holder and a home-assembled diffractometer that allows the recording of both small and wide-angle X-ray diffraction,[12] using a multilayer mirror (OSMIC-Rigaku, Troy, Michigan) and two position-sensitive small-angle detectors (HECUS-Braun, Graz, Austria). Recording of both small- and wide-angle X-ray diffraction was performed at room temperature. Small- and wide-angle patterns were recorded as a function of temperature between 10°C and 65°C on the Austrian beamline of Elettra (Trieste, Italy) together with differential scanning calorimetry measurements at heating and cooling rates of 1°C min^{-1} using similar samples. In both experiments, the detectors were calibrated at small and wide angles with high-purity tristearin and silver behenate, respectively.[11] The scattered intensity was reported as a function of the scattering vector $q = 4\pi \cdot \sin\theta/\lambda$, where θ is half the scattering angle and λ the X-ray wavelength.

Molecular modeling: A 2D structure of 4-(*N*)-trisnorsqualenoylgemcitabine created using ChemDraw was converted to a 3D model using Chem3D to generate the initial structure. All calculations were performed subsequently using Gaussian03 (Gaussian, Inc.).[9] The initial structure was energy-minimized using the AM1 and Polak–Ribiere conjugated gradient method. The termination condition was based on a root mean square (RMS) gradient of 0.001 kcal $Å^{-1}$ mol^{-1}. A Langevin dynamics simulation was performed over a 500 ps run time at a constant temperature of 300 K with a step size of 0.001 ps, a bath relaxation time of 0.1 ps, and a friction coefficient of 1. Conformers were sampled every 5 ps and energy-minimized as above. Two families of conformers were evidenced: the first with an extended conformation and the second with a bent U-shape conformation, both with relatively similar ΔHf. The energy minima of each family were then energy-minimized using a HTF quantum mechanics method and a 6-31G** basis set. In these conditions, the linear conformer was found to have a slightly energy-favored (binding energy difference: 1.2 kcal mol^{-1}). Using the low-energy extended conformer structure and the information obtained by X-ray diffraction, initially a disk-like assembly composed of 20 conjugates was created with the heterocyclic polar tetrahydrofuran moiety facing inwards and the squalene lipophilic side chain facing outwards. This system was too big to be calculated by AM1 in its totality. The system was thus energy-minimized (limited to 100 cycles) by pairs of conjugates going sequentially from one end to the other one. At the end of the process, the periodicity of the system was not lost, suggesting a good overall stability of the assembly. To challenge the stability of this supramolecular architecture, a Langevin dynamics simulation (using the same conditions as above) was performed, isolating a set of four molecules. After 50 ps of this process, the initial architecture was not greatly perturbed, confirming the overall stability of the system. Subsequently, a column system consisting of six superposed disks (i.e., 120 conjugates) was constructed and rapidly energy-minimized using the OPLS force field. A water spindle was then inserted in the polar core of the system. A virtual centroid inserted in the center of this spindle was used to adjust the distance (87.7 Å) between two water-filled columnar systems.[11]

In vivo anticancer activity: The animal experiments were carried out according to the principles of laboratory animal care and legislation in force in France. DBA/2 mice (4–5 weeks old) weighing about 15–18 g were used for the study. The mice were provided with standard mouse food and water ad libitum. The P388 leukemia subcutaneous tumour model was developed by injecting the exponentially growing P388 leukemia cells in suspension, containing 30% growth factor reduced Matrigel, subcutaneously (1×10^6 cells) at the lower abdominal portion of the mice. A palpable tumour was allowed to grow at the injection site. The tumour-bearing mice were divided into four groups of 7–8 mice each, that is, untreated, saline-treated, treated with gem (5 mg kg^{-1}), and treated with SQgem nanoassemblies (equivalent to 5 mg kg^{-1} gem). Considering the starting day of treatment as day 0, the three latter groups were intravenously treated on days 0, 4, 8, and 13. The mice were monitored regularly for differences in tumour volume and survival to assess the anticancer efficacy.

Determination of S-phase of cell cycle and apoptosis: To assess the in vivo anticancer efficacy of SQgem nanoassemblies versus gem by mechanistic means, the P388 wt ascitic model was developed by injecting 1×10^6 cells intraperitoneally into a DBA/2 mouse. After the development of palpable ascites, either gem (10 mg kg^{-1}) or SQgem nanoassemblies (10 mg kg^{-1} equivalent of gem) was injected intravenously into the ascitic mice. At day 3 post-injection, the ascitic fluid was collected from the peritoneal cavity of mice and processed for cell-cycle analysis and apoptosis. Cell-cycle events and apoptosis were determined by flow-cytometric measurements of cellular DNA content using the DNA-intercalating fluorochrome, propidium iodide (PI). Briefly, the collected ascitic cells were washed once with pH 7.4 phosphate-buffered saline (PBS) (2 mL). 1×10^6 cells were fixed overnight in 70% ethanol. The cells were centrifuged to remove ethanol, washed with PBS, and treated with extraction buffer (a mixture of 192 parts of 0.2 M di-

NANO MICRO small

sodium hydrogen phosphate and 8 parts of 0.1 M citric acid). Cells were then washed with PBS (2 mL) and treated with ribonuclease-A (200 $\mu g\,mL^{-1}$) for 30 min at 37°C. Subsequently, cells were stained with PI (50 $\mu g\,mL^{-1}$) in PBS. Measurements were made with a laser-based (488 nm) flow cytometer (FACS Calibur; Beckton and Dickenson, USA) and data acquired using the Cell Quest software (Beckton and Dickenson, USA). Off-line gating was performed using appropriate windows created by analysis of light scattering from untreated cells.

Acknowledgements

The authors wish to thank Dr. G. Barratt for her suggestions in preparing the manuscript, and acknowledge Gerard Pehau-Arnaudet for his support in using the 200 kV JEOL FEG 2010 electron microscope located at the Pasteur Institute, Paris. The financial support of the "Agence Nationale de la Recherche" (ANR, grant SYLIANU) and of the CNRS (grant "Ingénieur de valorisation") is acknowledged, as is the postdoctoral fellowship to L.H.R. from the Université Paris-Sud, France.

[1] L. Cattel, M. Ceruti, G. Balliano, F. Viola, in *Regulation of Isopentenoid Metabolism* (Eds: W. D. Nes, E. J. Parish, J. M. Trzaskos), American Chemical Society, Washington, D.C. **1992**, pp. 174–191.

[2] M. Ceruti, G. Balliano, F. Viola, G. Grosa, F. Rocco, L. Cattel, *J. Med. Chem.* **1992**, *35*, 3050–3058.

[3] L. Pogliani, M. Milanesio, M. Ceruti, D. Viterbo, *Chem. Phys. Lipids* **1999**, *103*, 81–93.

[4] R. Tilvis, P. T. Kovanen, T. A. Miettinen, *J. Biol. Chem.* **1982**, *257*, 10 300–10 305.

[5] P. Couvreur, B. Stella, L. H. Reddy, H. Hillaireau, C. Dubernet, D. Desmaële, S. Lepêtre-Mouelhi, F. Rocco, N. Dereuddre-Bosquet, P. Clayette, V. Rosilio, V. Marsaud, J.-M. Renoir, L. Cattel, *Nano Lett.* **2006**, *6*, 2544–2548.

[6] L. W. Hertel, G. B. Boder, J. S. Kroin, S. M. Rinzel, G. A. Poore, G. C. Todd, G. B. Grindey, *Cancer Res.* **1990**, *50*, 4417–4422.

[7] W. Plunkett, P. Huang, V. Gandhi, *Anticancer Drugs* **1995**, *6*, 7–13.

[8] D. Y. Bouffard, J. Laliberté, R. L. Momparler, *Biochem. Pharmacol.* **1993**, *45*, 1857–1861.

[9] M. J. Frisch, G. W. Trucks, H. B. Schlegel, G. E. Scuseria, M. A. Robb, J. R. Cheeseman, J. A. Montgomery, Jr., T. Vreven, K. N. Kudin, J. C. Burant, J. M. Millam, S. S. Iyengar, J. Tomasi, V. Barone, B. Mennucci, M. Cossi, G. Scalmani, N. Rega, G. A. Petersson, H. Nakatsuji, M. Hada, M. Ehara, K. Toyota, R. Fukuda, J. Hasegawa, M. Ishida, T. Nakajima, Y. Honda, O. Kitao, H. Nakai, M. Klene, X. Li, J. E. Knox, H. P. Hratchian, J. B. Cross, V. Bakken, C. Adamo, J. Jaramillo, R. Gomperts, R. E. Stratmann, O. Yazyev, A. J. Austin, R. Cammi, C. Pomelli, J. W. Ochterski, P. Y. Ayala, K. Morokuma, G. A. Voth, P. Salvador, J. J. Dannenberg, V. G. Zakrzewski, S. Dapprich, A. D. Daniels, M. C. Strain, O. Farkas, D. K. Malick, A. D. Rabuck, K. Raghavachari, J. B. Foresman, J. V. Ortiz, Q. Cui, A. G. Baboul, S. Clifford, J. Cioslowski, B. B. Stefanov, G. Liu, A. Liashenko, P. Piskorz, I. Komaromi, R. L. Martin, D. J. Fox, T. Keith, M. A. Al-Laham, C. Y. Peng, A. Nanayakkara, M. Challacombe, P. M. W. Gill, B. Johnson, W. Chen, M. W. Wong, C. Gonzalez, J. A. Pople, GAUSSIAN03, Revision C.02, Gaussian, Inc., Pittsburgh, PA **2003**.

[10] J. Ernst, W. S. Sheldrick, J.-H. Fuhrhop, *Angew. Chem. Int. Ed. Engl.* **1976**, *15*, 778.

[11] J. M. Seddon, J. Robins, T. Gulik-Krzywicki, H. Delacroix, *Phys. Chem. Chem. Phys.* **2000**, *2*, 4485–4493.

[12] M. Ollivon, G. Keller, C. Bourgaux, D. Kalnin, P. Villeneuve, P. Lesieur, *J. Therm. Anal. Calor.* **2006**, *83*, 219–224.

Received: August 21, 2007

